The Keller-Segel model with logistic sensitivity function and small diffusivity

Yasmin Dolak* Christian Schmeiser*,†

April 25, 2005

Abstract

The Keller-Segel model is the classical model for chemotaxis of cell populations. It consists of a drift-diffusion equation for the cell density coupled to an equation for the chemoattractant. Here a variant of this model is studied in one-dimensional position space, where the chemotactic drift is turned off for a limiting cell density by a logistic term and where the chemoattractant density solves an elliptic equation modeling a quasistationary balance of reaction and diffusion with production of the chemoattractant by the cells. The case of small cell diffusivity is studied by asymptotic and numerical methods. On a time scale characteristic for the convective effects, convergence of solutions to weak entropy solutions of the limiting nonlinear hyperbolic conservation law is proven. Numerical and analytic evidence indicates that solutions of this problem converge to irregular patterns of cell aggregates separated by entropic shocks from vacuum regions as time tends to infinity. Close to each of these patterns an 'almost' stationary solution of the full parabolic problem can be constructed up to an exponentially small (in terms of the cell diffusivity) residual. Based on a metastability hypothesis, the methods of exponential asymptotics are used to derive systems of ordinary differential equations approximating the long time behaviour of the parabolic problem on exponentially large time scales. The observed behavior is a coarsening process reminiscent of phase change models. A hybrid asymptotic-numerical approach for its simulation is introduced and its accuracy is shown by comparison to numerical simulations of the full problem.

Keywords: Chemotaxis, hyperbolic limit, entropy solution, exponential asymptotics

AMS subject classification: 35K55, 35K65, 35B40

*Johann Radon Institute for Computational and Applied Mathematics, Austrian Academy of Sciences, Altenbergerstr. 69, 4040 Linz, Austria.

†Institute for Analysis and Scientific Computing, TU Wien, Wiedner Hauptstr. 8-10, 1040 Wien, Austria.

1 Introduction

Chemotaxis, the active motion of organisms influenced by chemical gradients, has been studied both experimentally and theoretically by a large number of authors. The first mathematical model for chemotaxis was derived by Patlak [11], Keller and Segel [6]. In its most widely used formulation, the cell density $\varrho(x,t)$ at position $x \in \mathbb{R}^n$ and time $t > 0$ solves the convection diffusion equation

$$\partial_t \varrho + \nabla \cdot (\chi(\varrho, S)\varrho \nabla S - D(\varrho, S)\nabla \varrho) = 0. \tag{1}$$

This equation is coupled to an equation for the chemical concentration $S(x,t)$, typically a parabolic or elliptic equation with a reaction term describing production and degradation of the chemoattractant.

The Keller-Segel model has been applied to many different problems, ranging from bacterial chemotaxis to cancer growth or the immune response of the body. For some applications, it turns out that the diffusivity of cells plays only a minor role. In Dolak and Schmeiser [3], a convection equation with a small diffusion term as higher order correction is derived from a kinetic model for chemotaxis. Taking this case as a motivation, we will study a Keller-Segel model with a small diffusion constant and its limit of vanishing diffusivity. More precisely, we investigate

$$\partial_t \varrho + \partial_x(\chi(\varrho)\varrho \partial_x S) = D\partial_x^2 \varrho, \tag{2}$$

with $x \in (0, L)$ and $t > 0$. We assume the diffusion D to be constant and the chemotactic sensitivity $\chi(\varrho)$ to be of the form

$$\chi(\varrho) = \chi_0 \left(1 - \frac{\varrho}{\varrho_{max}}\right), \tag{3}$$

the maximal cell density ϱ_{max} and χ_0 being positive constants. Thus, the chemotactic response of the cells is shut off when a maximal density is reached. Models of this type have been first investigated by Hillen and Painter in [5]. In [10], the authors derive a chemotaxis model comprising a chemotactic sensitivity of the above form from a master-equation describing a random walk on a one-dimensional lattice by taking into account the finite size of cells.

The evolution of the chemoattractant S is described by

$$\partial_x^2 S = \beta S - \alpha \varrho. \tag{4}$$

This elliptic equation, instead of the more frequently used parabolic equation, is appropriate if we assume that diffusion of the chemoattractant is large in relation to the characteristic time and length scales of the problem.

We non-dimensionalize the equations (2) and (4) by choosing reference values for time, length, cell density and the chemical concentration, respectively:

$$x_0 = \frac{1}{\sqrt{\beta}}, \quad t_0 = \frac{1}{\alpha \chi_0 \varrho_{max}}, \quad \varrho_0 = \varrho_{max}, \quad S_0 = \frac{\alpha \varrho_{max}}{\beta}.$$

By introducing the dimensionless quantities

$$\bar{x} = \frac{x}{x_0}, \quad \bar{t} = \frac{t}{t_0}, \quad \bar{\varrho} = \frac{\varrho}{\varrho_0} \quad \text{and} \quad \bar{S} = \frac{S}{S_0}$$

and immediately dropping the bars, we obtain the non-dimensionalized system

$$\partial_t \varrho + \partial_x(\varrho(1-\varrho)\partial_x S) = \varepsilon \partial_x^2 \varrho \tag{5}$$

$$\partial_x^2 S = S - \varrho. \tag{6}$$

The only remaining dimensionless parameter is now

$$\varepsilon = \frac{D\beta}{\alpha \chi_0 \varrho_{max}}.$$

and in the following, we will shall assume $\varepsilon \ll 1$. This corresponds to a situation where the cells react to chemotactic signals strongly enough such that their velocity distribution is significantly biased towards the chemoattractant gradient as opposed to the case where unbiased reorientation dominates the behaviour of individual cells. In such a situation, a small diffusion term can be derived as a correction to the purely convective macroscopic limit of a kinetic transport model (see, e.g., [3], as mentioned above).

The initial condition is given by

$$\varrho(x,0) = \varrho_I^\varepsilon \,. \tag{7}$$

We choose homogeneous Neumann boundary conditions, i.e.

$$\partial_x \varrho(0,t) = \partial_x \varrho(L,t) = 0, \quad \partial_x S(0,t) = \partial_x S(L,t) = 0. \tag{8}$$

In the next section, we will analyze the limit $\varepsilon \to 0$ of system (5), (6). By deriving estimates which are uniformly valid for $\varepsilon > 0$, we will, by a compactness argument, show convergence of ϱ and S to entropy solutions of the corresponding hyperbolic system,

$$\partial_t \bar{\varrho} + \partial_x(\bar{\varrho}(1-\bar{\varrho})\partial_x \bar{S}) = 0, \tag{9}$$

$$\partial_x^2 \bar{S} = \bar{S} - \bar{\varrho}, \tag{10}$$

with

$$\partial_x \bar{S}(0,t) = \partial_x \bar{S}(L,t) = 0 \tag{11}$$

and subject to the initial condition

$$\bar{\varrho}(x,0) = \bar{\varrho}_I. \tag{12}$$

As a consequence of (11), the characteristics of (9) are parallel to the boundary and no boundary conditions for $\bar{\varrho}$ are needed.

In sections 3 and 4, we study the long time behaviour of solutions of the hyperbolic and the full parabolic system, respectively. In the latter, the formation of so-called pseudo-stationary or metastable states can be observed. We will use formal asymptotic methods to derive a system of ordinary differential equations describing the exponentially slow movement of these patterns. Finally, in section 5, we will investigate the long-time behaviour of solutions numerically. The metastability analysis is strongly related to recent work by Potapov and Hillen [13]. However, different scaling assumptions are used there and, consequently, a direct comparison of results is not straightforward.

2 Convergence of Solutions

In this section, we investigate the limit $\varepsilon \to 0$ in (5), (6), (7), (8). A similar problem from semiconductor physics is considered in Markowich and Szmolyan [8]. There, however, the non-linearity of the flux is only due to a coupling with an electric field (the equivalent to the chemical concentration here), and the formation of shocks in the hyperbolic problem is not observed.

The equations (5), (6) differ from the system analyzed in Hillen and Painter [5] by the fact that an elliptic instead of a parabolic equation for S is considered here. In [5] existence of an invariant region for (ϱ, S) in $\mathbb{R}^2$ and, consequently, global existence of smooth solutions is shown. In our case, the proof (based on a straightforward maximum principle) is much simpler and presented below for completeness.

We make the following assumption on the initial data:

$$\text{(A1)} \quad 0 \le \varrho_I^\varepsilon \le 1\,, \quad \varrho_I^\varepsilon \in W^{1,1}(0,L)\,, \quad \text{uniformly in } \varepsilon.$$

Theorem 2.1 *Let assumption (A1) hold. Then there exists a unique, global, smooth solution of (5), (6), (7), (8) satisfying*

$$0 \le \varrho(x,t),\ S(x,t) \le 1 \quad \textit{and} \quad \int_0^L \varrho(x,t)\,dx = \int_0^L \varrho_I(x)\,dx \tag{13}$$

and

$$S \in L^\infty((0,\infty); W^{2,\infty}(0,L)), \tag{14}$$

uniformly in ε as $\varepsilon \to 0$.

Proof. With the Greens's function

$$G(x,y) = \frac{1}{2}e^{-|x-y|} + \frac{e^{x+y} + e^{2L-x-y} + e^{x-y} + e^{y-x}}{2(e^{2L}-1)}\,, \tag{15}$$

the chemoattractant density can be computed from (6), (8), in terms of the cell density:

$$S(x,t) = \mathcal{S}[\varrho](x,t) := \int_0^L G(x,y)\varrho(y,t)dy\,. \tag{16}$$

Using this in (5), the resulting equation

$$\partial_t \varrho = \varepsilon \partial_x^2 \varrho - \partial_x(\varrho(1-\varrho)\partial_x \mathcal{S}[\varrho])$$

falls into the class of abstract semilinear parabolic equations. Local existence of unique, smooth solutions can be shown by semigroup techniques [12]. Then global existence follows from a comparison principle: writing (5) as

$$\partial_t \varrho + (2\varrho - 1)\partial_x S \partial_x \varrho + \varrho(1-\varrho)(S-\varrho) = \varepsilon \partial_x^2 \varrho,$$

it follows immediately that $\varrho = 0$ and $\varrho = 1$ are lower and upper solutions, respectively. A uniform (in time) bound for S is an obvious consequence of (16). □

We continue with estimates for the derivatives of ϱ.

Lemma 2.2 *Let assumption (A1) hold. Then the solution of (5)-(8) satisfies*

$$\varrho \in L^\infty_{loc}((0,\infty); W^{1,1}(0,L)), \text{ uniformly in } \varepsilon.$$

Proof. Differentiation of (5) with respect to x yields

$$\partial_t \partial_x \varrho + \partial_x((1-2\varrho)\partial_x\varrho\partial_x S + \varrho(1-\varrho)\partial_x^2 S) = \varepsilon\partial_x^3\varrho. \tag{17}$$

We define an approximation of the sign function by $\sigma_\delta(z) = \sigma(z/\delta)$, $0 < \delta \ll 1$, with σ smooth, increasing, $\sigma(0) = 0$ and $\sigma(z) = \operatorname{sign} z$ for $|z| > z_0$. Then, with $\operatorname{abs}_\delta(z) := \int_0^z \sigma_\delta(\xi)d\xi$, the convergence of $\operatorname{abs}_\delta(z)$ to $|z|$ as $\delta \to 0$ is uniform in $z \in \mathbb{R}$. Multiplying (17) with $\sigma_\delta(\partial_x\varrho)$ and integrating with respect to x yields

$$\begin{aligned}\int_0^L \sigma_\delta(\partial_x\varrho)\partial_t\partial_x\varrho\,dx + \int_0^L \sigma_\delta(\partial_x\varrho)\partial_x(\partial_x\varrho\partial_x S(1-2\varrho))\,dx \\ + \int_0^L \sigma_\delta(\partial_x\varrho)\partial_x(\varrho(1-\varrho)(S-\varrho))\,dx = \varepsilon\int_0^L \sigma_\delta(\partial_x\varrho)\partial_x^3\varrho\,dx.\end{aligned} \tag{18}$$

We integrate (18) by parts. The boundary terms vanish and we obtain

$$\begin{aligned}\frac{d}{dt}\int_0^L \operatorname{abs}_\delta(\partial_x\varrho)\,dx - \int_0^L \sigma_\delta'(\partial_x\varrho)\partial_x\varrho\partial_x^2\varrho\partial_x S(1-2\varrho)\,dx \\ + \int_0^L \sigma_\delta(\partial_x\varrho)\partial_x(\varrho(1-\varrho)(S-\varrho))\,dx = -\varepsilon\int_0^L \sigma_\delta'(\partial_x\varrho)(\partial_x^2\varrho)^2\,dx \le 0.\end{aligned} \tag{19}$$

The function $f_\delta(z) = \sigma_\delta(z)z - \operatorname{abs}_\delta(z)$ satisfies $f_\delta'(z) = \sigma_\delta'(z)z$ and converges to 0 uniformly in $z \in \mathbb{R}$. We integrate the second term in (19) by parts, which gives

$$\frac{d}{dt}\int_0^L \operatorname{abs}_\delta(\partial_x\varrho)\,dx \le -\int_0^L f_\delta(\partial_x\varrho)\partial_x(\partial_x S(1-2\varrho))\,dx - \int_0^L \sigma_\delta(\partial_x\varrho)\partial_x(\varrho(1-\varrho)(S-\varrho))\,dx. \tag{20}$$

The last term can be estimated by

$$\begin{aligned}-\int_0^L \sigma_\delta(\partial_x\varrho)\partial_x(\varrho(1-\varrho)(S-\varrho))\,dx = -\int_0^L \sigma_\delta(\partial_x\varrho)\varrho(1-\varrho)\partial_x S\,dx \\ -\int_0^L \sigma_\delta(\partial_x\varrho)\partial_x\varrho(3\varrho^2 - 2\varrho(S+1) + S)\,dx \le c_1 + c_2\int_0^L |\partial_x\varrho|\,dx.\end{aligned}$$

In the limit $\delta \to 0$, the first term of the right hand side of (20) vanishes and we obtain

$$\frac{d}{dt}\int_0^L |\partial_x\varrho|\,dx \le c_1 + c_2\int_0^L |\partial_x\varrho| dx. \tag{21}$$

The assertion of lemma 2.2 now follows from the Gronwall inequality. □

Lemma 2.3 *Let (A1) hold. Then the solution of (5)-(8) satisfies*

$$\sqrt{\varepsilon}\partial_x \varrho, \partial_t \partial_x S \in L^2_{loc}((0,\infty)\times[0,L]), \quad \textit{uniformly in } \varepsilon.$$

Proof. We write (5) as

$$\partial_t \varrho = \partial_x(\varepsilon \partial_x \varrho - \varrho(1-\varrho)\partial_x S). \tag{22}$$

Multiplication by ϱ and integration with respect to x leads to

$$\frac{1}{2}\frac{d}{dt}\int_0^L \varrho^2\,dx + \varepsilon\int_0^L (\partial_x\varrho)^2\,dx = \int_0^L \varrho(1-\varrho)\partial_x S \partial_x \varrho\,dx. \tag{23}$$

Since the integrand in the last term is in $L^1((0,L))$ uniformly in t and ε by the previous result, we obtain the boundedness of $\sqrt{\varepsilon}\partial_x\varrho$ by integration with respect to t. As a consequence, the flux density $J = \varrho(1-\varrho)\partial_x S - \varepsilon\partial_x\varrho$ is also uniformly bounded in $L^2_{loc}((0,\infty)\times[0,L])$. Differentiating equation (6) with respect to x and t and using $\partial_t\varrho + \partial_x J = 0$, we obtain

$$\partial_t\partial_x^3 S - \partial_t\partial_x S = \partial_x^2 J.$$

Thus, $\partial_t\partial_x S = -\mathcal{S}[\partial_x^2 J]$. Since the expression on the right hand side is a bounded operator applied to $J \in L^2_{loc}((0,\infty)\times[0,L])$, the proof is complete. □

Theorem 2.4 *Let the assumption (A1) hold, (ϱ, S) be a solution of (5) - (8), and $T > 0$. Then, as $\varepsilon \to 0$ (restricting to subsequences),*

$$\varrho \to \bar\varrho \text{ in } C([0,T];L^1((0,L))) \quad \textit{and} \quad S \to \bar S \text{ in } C([0,T];C^1([0,L])). \tag{24}$$

The limit $(\bar\varrho, \bar S) \in L^\infty((0,T);BV((0,L))\times W^{2,\infty}((0,L)))$ solves (9), (10), (11), where $\bar\varrho_I \in BV((0,L))$ is an accumulation point of ϱ_I^ε. Moreover, $\bar\varrho$ is an entropy solution of (9), i.e.

$$\partial_t\eta(\bar\varrho) + \partial_x(\psi(\bar\varrho)\partial_x\bar S) + (\bar\varrho(1-\bar\varrho)\eta'(\bar\varrho) - \psi(\bar\varrho))(\bar S - \bar\varrho) \le 0 \tag{25}$$

holds in the weak sense for every smooth, convex η and with $\psi'(\bar\varrho) = (1-2\bar\varrho)\eta'(\bar\varrho)$.

Remark: Note that the entropy inequality does not give rise to a decaying entropy functional.

Proof. The boundedness of the flux density (proof of lemma 2.3) gives $\partial_t\varrho \in L^2((0,T);H^{-1}((0,L))$. Together with lemma 2.2 this implies that ϱ is in a compact set in $C([0,T];L^1((0,L)))$ (see Simon [15]). From theorem 2.1, lemma 2.3 and an anisotropic generalization of the Sobolev embedding of $W^{1,p}$ in $C^{0,1-n/p}$, $p > n$ (see Haskovec and Schmeiser [4]), it follows that $\partial_x S$ is uniformly bounded in $C^{0,1/3}([0,T]\times\bar\Omega)$, $T > 0$. An application of the Arzela-Ascoli theorem concludes the proof of (24). The strong convergence of ϱ and $\partial_x S$ allows to pass to the limit in the weak formulation of (5)-(8) giving the weak formulation of (9)-(11) for $\bar\varrho$ and $\bar S$. The entropy inequality (25) follows analogously. □

3 Long-time behaviour of the hyperbolic system

In this section, we investigate the stability and the asymptotic behaviour of entropy solutions of the hyperbolic system. Stationary solutions of (9), (10), (11) satisfy

$$\begin{aligned} \bar{\varrho}(1-\bar{\varrho})\partial_x \bar{S} &= 0 \qquad (26)\\ \partial_x^2 \bar{S} &= \bar{S} - \bar{\varrho}. \qquad (27) \end{aligned}$$

It can be immediately seen that $\bar{\varrho} = \bar{S} = const$ is a solution.

Lemma 3.1 *The constant solution, $\bar{\varrho} = \bar{S} = \frac{m}{L}$, where $0 < m < L$ is the total mass, of system (9), (10), (11) is unstable.*

Proof. We multiply (9) by $\bar{S}$ and differentiate (10) with respect to t to obtain

$$\frac{1}{2}\frac{d}{dt}\int_0^L (\bar{S}^2 + (\partial_x \bar{S})^2)dx = \int_0^L \bar{\varrho}(1-\bar{\varrho})(\partial_x \bar{S})^2 dx. \qquad (28)$$

For small non constant perturbations, the right hand side of this equation is positive $\forall\ t$, hence $\int_0^L (\bar{S}^2 + (\partial_x \bar{S})^2)dx$ is increasing in time. We rearrange this integral by writing

$$\begin{aligned} \int_0^L (\bar{S}^2 + (\partial_x \bar{S})^2)dx &= \int_0^L \Big[\Big(\frac{m}{L} + \bar{S} - \frac{m}{L}\Big)^2 + (\partial_x \bar{S})^2\Big]dx \qquad (29)\\ &= \frac{m^2}{L} + 2\int_0^L \frac{m}{L}\Big(\bar{S} - \frac{m}{L}\Big)dx + \int_0^L \Big[\Big(\bar{S} - \frac{m}{L}\Big)^2 + (\partial_x \bar{S})^2\Big]dx. \end{aligned}$$

Since the total mass is conserved, we consider only perturbations with mass 0. Thus, we have $\int_0^L \bar{S}\,dx = \int_0^L \bar{\varrho}\,dx = m\ \ \forall\ t$, and the second term on the right hand side vanishes. Hence,

$$\min_{\int \bar{S}dx = m} \int_0^L \Big(\bar{S}^2 + (\partial_x \bar{S})^2\Big)dx = \frac{m^2}{L},$$

which is only achieved for $\bar{S} = \frac{m}{L}$. As the integral on the left hand side is increasing in time, lemma 3.1 follows. □

Lemma 3.2 *As $t \to \infty$, $\bar{\varrho}(1-\bar{\varrho})(\partial_x \bar{S})^2 \to 0$ in the following sense:*

$$\int_\tau^\infty \int_0^L \bar{\varrho}(1-\bar{\varrho})(\partial_x \bar{S})^2 dx\,dt \xrightarrow{\tau\to\infty} 0. \qquad (30)$$

Proof. Integration of (28) from $t = 0$ to ∞ shows that

$$\int_0^\infty \int_0^L \bar{\varrho}(1-\bar{\varrho})(\partial_x \bar{S})^2 dx dt < \infty, \qquad (31)$$

which implies the assertion. □

From this, and the steady state equations (26), (27), we expect convergence to piecewise

constant steady states, with $\bar{\varrho} = 0$, $\bar{\varrho} = 1$ or $\bar{S}_x = 0$. Going back to the time-dependent problem (9), (10) and applying the method of characteristics, we find that along characteristics given by $\dot{x} = (1 - 2\bar{\varrho})\partial_x \bar{S}$, $\bar{\varrho}$ evolves according to $\dot{\bar{\varrho}} = (\bar{\varrho} - \bar{S})\bar{\varrho}(1 - \bar{\varrho})$. It immediately follows that $\bar{\varrho} = \bar{S} = const$, with $0 < const < 1$, is unstable. If $\bar{\varrho}$ gets sufficiently small such that $\bar{S} > \bar{\varrho}$, then $\bar{\varrho} = 0$ is attracting, and a similar argument holds for $\bar{\varrho} = 1$. Hence, we expect solutions to approach (as $t \to \infty$) functions of the form

$$\bar{\varrho}_\infty(x) = \frac{1 - (-1)^{k_i}}{2} \qquad \text{for } x_i < x < x_{i+1}\,, \tag{32}$$

with $0 = x_0 < x_1 < ... < x_{M+1} = L$, $k_i = k_0 + i$, and

$$\bar{S}_\infty = \mathcal{S}[\bar{\varrho}_\infty]\,. \tag{33}$$

Plateaus where $\bar{\varrho}_\infty = 1$ alternate with vacuum regions ($\bar{\varrho}_\infty = 0$). At the left, it starts with a plateau for $k_0 = 1$, or with a vacuum region for $k_0 = 0$. The union of all plateau regions is denoted by

$$P = \bigcup_{k_i \text{ odd}} (x_i, x_{i+1})\,.$$

It follows from mass conservation that

$$l(P) = \sum_{k_i \text{ odd}} (x_{i+1} - x_i) = \int_0^L \bar{\varrho}_I \, dx.$$

Not all possible stationary solutions $\bar{\varrho}_\infty$ are indeed entropy solutions. For scalar conservation laws the sign of the jump of the density $\bar{\varrho}_\infty$ at an entropic shock is related to the convexity behaviour of the flux $\bar{\varrho}_\infty(1 - \bar{\varrho}_\infty)\partial_x \bar{S}_\infty$. This leads to a condition on the sign of $\partial_x \bar{S}_\infty$ at the plateau edges:

$$(-1)^{k_i} \bar{S}_{\infty,x}(x_i) < 0, \quad 1 \le i \le M. \tag{34}$$

Formally, $\partial_x \bar{S}_\infty$ would also be allowed to be zero. Such a solution would however be unstable, since a small perturbation would lead to a violation of the entropy condition. A possible derivation of (34) is given in the following section by the construction of shock profiles for the full parabolic problem, i.e., boundary layer solutions smoothing the jumps of $\bar{\varrho}_\infty$.

Next, we investigate the stability of the stationary solution $(\bar{\varrho}_\infty, \bar{S}_\infty)$ with respect to a particular class of perturbations. We introduce the initial data

$$\bar{\varrho}_I(x) = \frac{1 - (-1)^{k_i}}{2} + \varepsilon u_I(x) \qquad \text{for } x \in (x_i + \varepsilon\xi_i(0), x_{i+1} + \varepsilon\xi_{i+1}(0)) = I_i(0)\,, \tag{35}$$

where u_I is a piecewise smooth function and $|\varepsilon| \ll 1$. Then, solutions of (9), (10) have jumps at $x_i + \varepsilon\xi_i(t)$, and

$$\bar{\varrho}(x,t) = \frac{1 - (-1)^{k_i}}{2} + \varepsilon u(x,t) \qquad \text{for } x \in (x_i + \varepsilon\xi_i(t), x_{i+1} + \varepsilon\xi_{i+1}(t)) = I_i(t)\,. \tag{36}$$

The Rankine-Hugoniot jump condition reads

$$\varepsilon\dot{\xi}_i[\bar{\varrho}] = [\bar{\varrho}(1-\bar{\varrho}]\partial_x\bar{S}\Big|_{x=x_i+\varepsilon\xi_i}$$

which, at leading order, yields

$$\dot{\xi}_i(t) = -\left(u(x_i+,t) + u(x_i-,t)\right)\bar{S}_{\infty,x}(x_i).$$

Using (36) in (9), it follows that $u(x,t)$ approximately satisfies

$$\begin{aligned} \partial_t u - \partial_x(u\partial_x\bar{S}_\infty) &= 0 \qquad \text{in } P\,, \\ \partial_t u + \partial_x(u\partial_x\bar{S}_\infty) &= 0 \qquad \text{in } Z := (0,L)\setminus P\,. \end{aligned}$$

By the method of characteristics, we derive

$$\dot{x} = -\partial_x\bar{S}_\infty, \quad \dot{u} = u\partial_x^2\bar{S}_\infty = u(\bar{S}_\infty - 1) \qquad \text{in } P\,,$$

$$\dot{x} = \partial_x\bar{S}_\infty, \quad \dot{u} = -u\partial_x^2\bar{S}_\infty = -u\bar{S}_\infty \qquad \text{in } Z.$$

Since $\bar{S}_\infty$ is concave in P and convex in Z, exactly one extremum $\bar{x}_{i+1/2}$ exists between x_i and x_{i+1} for $1 \le i \le M-1$. Since the derivative of $\bar{S}_\infty$ also vanishes at the boundary points, we introduce the notation $\bar{x}_{1/2} := 0$, $\bar{x}_{M+1/2} = L$. All of the characteristics except those starting at $\bar{x}_{i+1/2}$, $0 \le i \le M$, go into one of the x_i, and u decays along characteristics. The limit of the length of the plateau $I_i(t)$ (k_i odd) as $t \to \infty$ is given by

$$\begin{aligned} l(I_i(\infty)) &= l(I_i(0)) + \varepsilon\int_0^\infty \left(\dot{\xi}_{i+1} - \dot{\xi}_i\right) dt \\ &= l(I_i(0)) + \varepsilon\int_0^\infty [-(u\partial_x\bar{S}_\infty)(x_{i+1}+) - (u\partial_x\bar{S}_\infty)(x_{i+1}-) \\ &\quad + (u\partial_x\bar{S}_\infty)(x_i+) + (u\partial_x\bar{S}_\infty)(x_i-)]dt \\ &= l(I_i(0)) - \varepsilon\int_0^\infty\int_{x_i}^{x_{i+1}} \partial_x(u\partial_x\bar{S}_\infty)dxdt + \varepsilon\int_0^\infty\int_{x_{i+1}}^{\bar{x}_{i+3/2}} \partial_x(u\partial_x\bar{S}_\infty)dxdt \\ &\quad + \varepsilon\int_0^\infty\int_{\bar{x}_{i-1/2}}^{x_i} \partial_x(u\partial_x\bar{S}_\infty)dxdt \\ &= l(I_i(0)) - \varepsilon\left(\int_{x_i}^{x_{i+1}} u\,dx + \int_{x_{i+1}}^{\bar{x}_{i+3/2}} u\,dx + \int_{\bar{x}_{i-1/2}}^{x_i} u\,dx\right)_{t=0}^{\infty} \end{aligned}$$

Since $u \xrightarrow{t\to\infty} 0$, we obtain

$$l(I_i(\infty)) = l(I_i(0)) + \varepsilon\int_{\bar{x}_{i-1/2}}^{\bar{x}_{i+3/2}} u_I dx. \tag{37}$$

Thus, as $t \to \infty$, each plateau attracts all the mass initially distributed between the neighbouring minima of $\bar{S}_\infty$. We can interpret this as a neutral stability of steady states

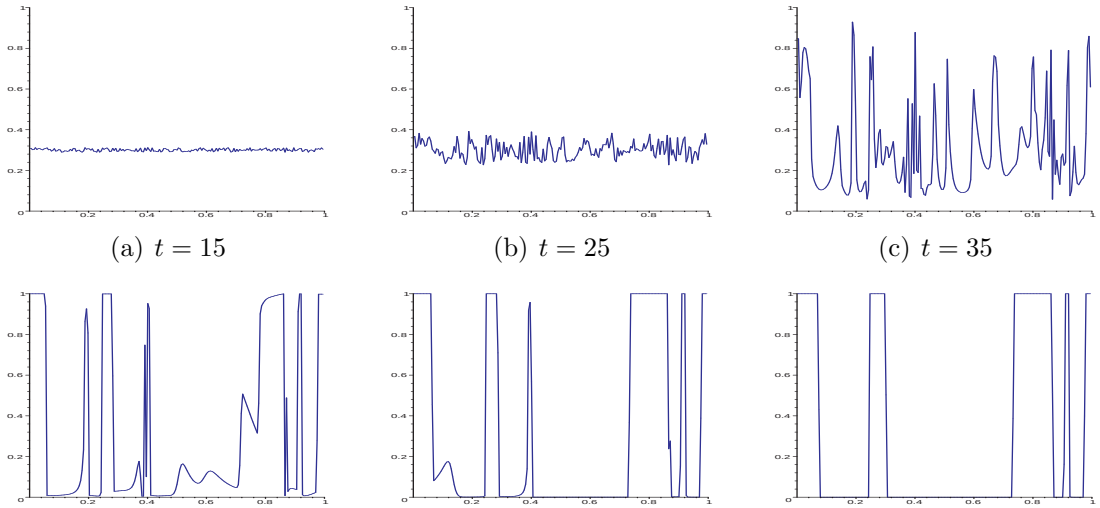

(a) $t = 15$ (b) $t = 25$ (c) $t = 35$

(d) $t = 45$ (e) $t = 60$ (f) $t = 100$

Figure 1: Temporal evolution of the cell density $\bar{\varrho}$, starting from random initial data $\bar{\varrho}_I \in [0.3, 0.31]$ and with $L = 1$.

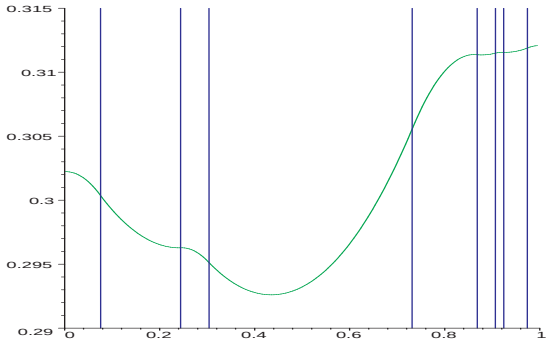

Figure 2: Cell density $\bar{\varrho}$ (dark) and chemical concentration $\bar{S}$ (light) at $t = 100$.

with alternating plateau and vacuum regions with respect to perturbations of the type (35).

In Fig. 1 and 2, we solved the problem (9) - (11) numerically. At each time step, first the new chemical concentration is calculated from the old cell density, then the cell density is updated using an upwind method. In Fig. 1, we can observe the formation of shocks and rarefaction waves, until, in the last picture, the stationary state is reached and no further movement of the plateaus can be observed. In Fig. 2, the corresponding chemical concentration $\bar{S}$ is shown. Note that as discussed above, the chemical follows the course of the cell density $\bar{\varrho}$, even in the case of the slim plateau on the right side of the domain.

4 Long-time behaviour of the parabolic system

In this section, we will be concerned with the stability and the asymptotic behaviour of solutions of the full parabolic problem (5)-(8). All stationary solutions have been characterized by Potapov and Hillen in [13] by a phase plane analysis. They are the restrictions of periodic solutions of the stationary differential equations to the interval $(0, L)$.

The dynamic problem studied in [13] differs from (5)–(8) by the fact that S is given by a parabolic equation. The authors show that all stationary solutions lie on branches bifurcating from the spatially uniform stationary solution in dependence of a bifurcation parameter inversely proportional to ε. It turns out that the constant solution is linearly stable for large enough diffusivity. After a first bifurcation its stability is transferred to a bifurcating solution. For the model (5)–(8), the linear stability result can be extended to global nonlinear stability.

Lemma 4.1 *Let assumption (A1) hold and let $\varepsilon > \frac{1}{4}$. Then the solution of (5)–(8) converges to the constant stationary solution as $t \to \infty$.*

Proof. Similarly to the proof of lemma 3.1, we multiply (5) by S and differentiate (6) with respect to t to obtain, after integration by parts of the last term on the right hand side,

$$\frac{1}{2}\frac{d}{dt}\int_0^L (S^2 + (\partial_x S)^2)dx = \int_0^L \varrho(1-\varrho)(\partial_x S)^2 dx - \varepsilon \int_0^L ((\partial_x S)^2 + (\partial_x^2 S)^2)dx. \qquad (38)$$

We can estimate the left hand side by

$$\begin{aligned} \frac{1}{2}\frac{d}{dt}\int_0^L (S^2 + (\partial_x S)^2)dx &= \int_0^L \varrho(1-\varrho)(\partial_x S)^2 dx - \varepsilon \int_0^L ((\partial_x S)^2 + (\partial_x^2 S)^2)dx \qquad (39) \\ &\leq \Big(\frac{1}{4} - \varepsilon\Big) \int_0^L ((\partial_x S)^2 + (\partial_x^2 S)^2)dx. \end{aligned}$$

For $\varepsilon > \frac{1}{4}$, the right hand side of (39) is negative. Integration from 0 to t yields

$$\int_0^L (\partial_x S)^2(x,t)\,dx \leq \Big(\frac{1}{2} - 2\varepsilon\Big) \int_0^t \int_0^L (\partial_x S)^2 dx + \int_0^L (S^2 + (\partial_x S)^2)dx\Big|_{t=0}.$$

Applying Gronwall's lemma, it follows that $\|\partial_x S\|_{L^2(0,L)} \to 0$ and as a consequence, $S \to const$ as $t \to \infty$. □

The result is sharp in the sense that a linear stability analysis yields $\varepsilon = \frac{1}{4}$ as the first bifurcation point, where the constant steady state looses its stability.

We motivate our study of the dynamics for small values of ε by presenting the result of a numerical experiment. Fig. 3 shows a numerical solution of (5)–(8) with $\varepsilon = 2\times 10^{-4}$. We used the same numerical scheme as in the previous section with an explicit discretization of the diffusion term. Starting from homogeneous initial data with small perturbations, a

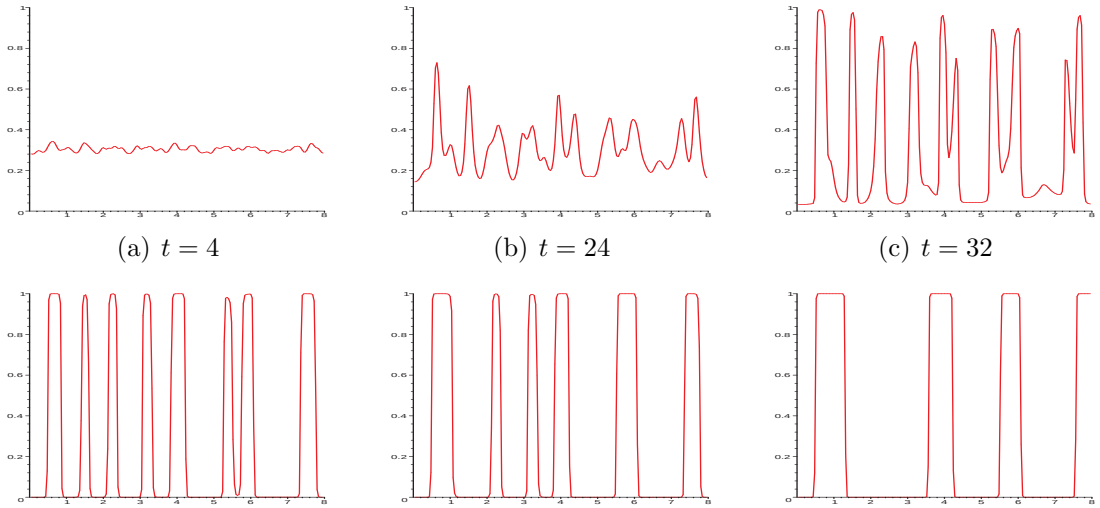

(a) $t = 4$ (b) $t = 24$ (c) $t = 32$

(d) $t = 56$ (e) $t = 800$ (f) $t = 8000$

Figure 3: Numerical solution of the parabolic system (5), (6) with random initial data $\varrho_I \in [0.3, 0.31]$, $L = 10$ and $\varepsilon = 2 \times 10^{-4}$.

pattern with several plateaus is formed as for the hyperbolic problem. Once this pattern has formed, it remains structurally stable for a long time, with the plateaus moving very slowly. Eventually, neighbouring plateaus merge with each other. This merging process occurs on a comparatively fast time scale. The new pattern, now with one peak less, undergoes the same coarsening process.

Experimentally, this so called metastable behaviour is a well known phenomenon in many fields, for instance solid-state physics. Mathematically, it has been studied in various contexts such as the movement of viscous shocks [7], [14] or the Cahn-Hillard equation (for instance [1] and [2]). A chemotaxis model featuring the formation of spike solutions is considered in [16].

The peculiar long-time behaviour of system (5), (6) can be interpreted as follows. Each pseudo-stationary state of the parabolic system is exponentially close to a stationary entropy solution of the hyperbolic system. In contrast to the latter however, the small diffusion allows plateaus to communicate with each other, and smaller plateaus are attracted by neighbouring larger ones producing more chemoattractant. The whole phenomenon depends on a non-zero diffusion coefficient ε. Eventually, plateaus will get so close to each other that in general, the corresponding stationary solutions of the hyperbolic system cannot satisfy the entropy condition any more. Then, a fast transition takes place and the smaller plateau merges with the larger one. On this fast time scale, solutions behave practically like in the hyperbolic case, and a smoothened version of a rarefaction wave can be observed.

After the two peaks have merged, it is again diffusion that dominates the behaviour. The whole process repeats itself, until only one single plateau is left, which will typically move to one of the domain boundaries. Thus, the only stable stationary state seems to be one plateau at the left or right boundary of the domain.

By construction of approximate solutions, it is shown numerically and analytically in [13] that the eigenvalues describing the slow movement of the peaks exponentially approach zero as the length of the domain increases. These exponentially small eigenvalues are typical features of metastable systems. The authors also derive an ODE describing the dynamics of a structure with two plateaus at the domain boundaries. Here, we will use exponential asymptotics to formally derive a system of ordinary differential equations describing the slow movement of the plateaus. This method has been successfully used in various applications, see for instance Ward [19] and references therein.

Metastable dynamics of the parabolic system

In the following analysis of the long-time behaviour of system (5), (6), now rewritten as

$$\partial_t \varrho + \partial_x J = 0\,, \qquad J = \varrho(1-\varrho)\partial_x \mathcal{S}[\varrho] - \varepsilon \partial_x \varrho\,, \qquad J = 0 \quad \text{at } x = 0, L\,, \tag{40}$$

we will assume that the formation of patterns from the initial data has already taken place, and that a quasi-stationary pattern with plateaus (close to (32)) has been formed. Our aim is to derive a system of equations describing the evolution of the positions of the plateau boundaries $x_1(t), \dots, x_M(t)$.

A first approximation to a solution of the parabolic problem with plateaus is a stationary entropy solution of the hyperbolic problem $(\bar\varrho_\infty, \bar S_\infty)$ solving (32) and (33). However, we need a much better approximation $(\tilde\varrho, \tilde S)$ with boundary layer corrections close to the jumps of $\bar\varrho_\infty$. Actually we shall try to solve the parabolic steady state problem

$$\varepsilon \partial_x \varrho - \varrho(1-\varrho)\partial_x \mathcal{S}[\varrho] = 0\,, \tag{41}$$

as precisely as possible. The approximation $\tilde S$ for the chemoattractant density will be constructed such that it is close to $\bar S_\infty$ with the same qualitative behaviour. In particular, it has the same monotonicity behaviour at the plateau boundaries and extrema $\tilde x_{i+1/2}$ with the ordering $0 = \tilde x_{1/2} < x_1 < \tilde x_{3/2} < \ldots < \tilde x_{M-1/2} < x_M < \tilde x_{M+1/2} = L$ as the extrema $\bar x_{i+1/2}$ of $\bar S_\infty$ introduced above. For the construction of the approximating cell density, we consider the boundary layer problem

$$\varepsilon \partial_x \hat\varrho_i = \hat\varrho_i(1-\hat\varrho_i)\partial_x \tilde S\,, \qquad \hat\varrho_i(x_i) = 1/2\,, \tag{42}$$

where the auxiliary condition fixes the position of the boundary layer. The solution

$$\hat\varrho_i[\tilde S](x) = \left[1 + \exp\left(\frac{\tilde S(x_i) - \tilde S(x)}{\varepsilon}\right)\right]^{-1} \tag{43}$$

will be used for $\tilde x_{i-1/2} < x < \tilde x_{i+1/2}$. The shape of $\hat\varrho_i$ depends on the monotonicity of $\tilde S$ in this interval: for increasing $\tilde S$, $\hat\varrho_i(\tilde x_{i-1/2}) \approx 0$ and $\hat\varrho_i(\tilde x_{i+1/2}) \approx 1$, and vice versa for decreasing $\tilde S$. Thus, the boundary layer solution has the appropriate behaviour for jumps satisfying the entropy condition (34).

The construction of the boundary layer solution is nonstandard from the point of view of singular perturbation theory, where the standard procedure would lead to evaluation

of $\partial_x \tilde{S}$ at $x = x_i$ in (42) and, consequently, $\hat{\varrho}_i[\tilde{S}](x) = \left[1 + \exp\left(\partial_x \tilde{S}(x_i)(x_i - x)/\varepsilon\right)\right]^{-1}$. This is, of course, an approximation of (43), obtained by Taylor expansion of $\tilde{S}$. The better accuracy of (43) is needed in the exponential asymptotics here.

By patching together the boundary layer solutions at the points $\tilde{x}_{i+1/2}$, exponentially small jump discontinuities would be created. By shifting the contributions appropriately, a continuous (actually continuously differentiable) approximate cell density is constructed:

$$\tilde{\varrho}[\tilde{S}](x) = \hat{\varrho}_i[\tilde{S}](x) - \Delta\varrho_i[\tilde{S}]\,, \qquad \text{for } \tilde{x}_{i-1/2} < x < \tilde{x}_{i+1/2} \tag{44}$$

with

$$\Delta\varrho_i[\tilde{S}] = \sum_{j=1}^{i-1} \left[\hat{\varrho}_{j+1}[\tilde{S}](\tilde{x}_{j+1/2}) - \hat{\varrho}_j[\tilde{S}](\tilde{x}_{j+1/2})\right].$$

Note again that these corrections are exponentially small as $\varepsilon \to 0$. There is a certain arbitrariness in their choice. They would also serve their purpose if they would all be shifted by the same constant, which could be fixed by prescribing the total mass, i.e. the total number of cells. However, since our final result will only contain differences of the $\Delta\varrho_i[\tilde{S}]$, this issue is not important for us.

Finally, we require the chemoattractant density to satisfy

$$\tilde{S} = \mathcal{S}[\tilde{\varrho}[\tilde{S}]]\,. \tag{45}$$

This is a highly nonlinear problem whose solvability is not trivial at all. In the appendix we prove, for small ε, existence of a unique solution close to $\bar{S}_\infty$ and satisfying the qualitative assumptions mentioned above. The fact that $(\tilde{\varrho}, \tilde{S})$ is completely determined by the positions $x_1, \ldots, x_M$ of the plateau boundaries motivates the notation $\tilde{\varrho} = \tilde{\varrho}(x; x_1, \ldots, x_M)$, $\tilde{S} = \tilde{S}(x; x_1, \ldots, x_M)$. If these coincide with the points where a stationary cell density takes the value $1/2$, then all the $\Delta\varrho_i$ vanish and $(\tilde{\varrho}, \tilde{S})$ is an exact steady state, since it also satisfies the Neumann boundary conditions $\partial_x \tilde{\varrho} = 0$, $x = 0, L$, by its construction and by the boundary conditions for $\tilde{S}$. In general, however, we obtain the residual

$$R := \varepsilon\partial_x\tilde{\varrho} - \tilde{\varrho}(1-\tilde{\varrho})\partial_x\tilde{S} = \Delta\varrho_i(1 - 2\hat{\varrho}_i + \Delta\varrho_i)\partial_x\tilde{S} \quad \text{in } (\tilde{x}_{i-1/2}, \tilde{x}_{i+1/2})\,. \tag{46}$$

The following procedure is an adaption of the methodology developed by Ward et al. for an asymptotic approximation of the metastable dynamics of the Ginzburg-Landau equation, viscous shocks, and the viscous Cahn-Hilliard equation (for an overview, see for instance [18]). The term 'metastable' can be made more precise by considering the linearization of the problem around the M-parameter family of approximate steady states. The exponential smallness of the residuals leads to expecting M exponentially small eigenvalues. Metastability means that all the other eigenvalues are nonnegative. We do not have any results on the spectral problem, but the assumption of metastability is strongly supported by our numerical experiments and, even stronger, by the numerical studies of the eigenvalue problem in [13].

We start by introducing a correction term for our approximate solution:

$$\varrho(x,t) = \tilde{\varrho}(x; x_1(t), ..., x_M(t)) + r(x,t)\,. \tag{47}$$

Since the approximate solution satisfies the boundary conditions, we have $\partial_x r = 0$ at $x = 0, L$. Just as in [18], we now consider an approximate version of (40), dropping nonlinear terms in r and assuming $|\partial_t r| \ll |\partial_t \tilde{\varrho}|$:

$$\partial_t \tilde{\varrho} + \partial_x J = 0\,, \qquad \mathcal{L} r + J + R = 0\,, \qquad J = 0 \quad \text{at } x = 0, L\,, \tag{48}$$

with the linearization of (41),

$$\mathcal{L} r = \varepsilon \partial_x r - (1 - 2\tilde{\varrho}) \partial_x \tilde{S} r - \tilde{\varrho}(1 - \tilde{\varrho}) \partial_x \mathcal{S}[r]\,. \tag{49}$$

The nonlocal term $\mathcal{S}[r]$ is one of the major differences to the work in the above mentioned references. As a first step, J will be computed by integrating the first equation in (48). From the definition of $\tilde{\varrho}$ in $(\tilde{x}_{i-1/2}, \tilde{x}_{i+1/2})$ we have

$$\partial_t \tilde{\varrho} = \frac{\hat{\varrho}_i(1 - \hat{\varrho}_i)}{\varepsilon} \left[-\partial_x \tilde{S}(x_i) \dot{x}_i + \sum_{j=1}^{M} \left(\partial_{x_j} \tilde{S}(x) - \partial_{x_j} \tilde{S}(x_i) \right) \dot{x}_j \right] - \sum_{j=1}^{M} \partial_{x_j} \Delta\varrho_i \dot{x}_j\,.$$

From the differential equation (42) for the boundary layer term $\hat{\varrho}_i$ we see that $\hat{\varrho}_i(1 - \hat{\varrho}_i)/\varepsilon$ is an approximate Delta-distribution concentrated at $x = x_i$ and with weight $|\partial_x \tilde{S}(x_i)|^{-1}$. The derivatives of the corrections $\Delta\varrho_i$ with respect to the x_j are expected to be exponentially small just as the $\Delta\varrho_i$ themselves. With these observations and (34), integration of the first equation in (48) gives

$$J(x) \approx \sum_{j=1}^{i} (-1)^{k_j} \dot{x}_j \qquad \text{for } x_i < x < x_{i+1}\,.$$

Here the boundary condition $J(0) = 0$ has been used. The other boundary condition $J(L) = 0$ leads to the equation

$$\sum_{j=1}^{M} (-1)^{k_j} \dot{x}_j = 0\,, \tag{50}$$

representing conservation of mass.

Now the second equation in (48) is multiplied by a test function $\psi(x, t)$ and integrated:

$$\varepsilon \psi r|_{x=0}^{L} + \int_0^L (r \mathcal{L}^* \psi + \psi(J + R)) dx = 0\,, \tag{51}$$

with the formally adjoint operator

$$\mathcal{L}^* \psi = -\varepsilon \partial_x \psi - (1 - 2\tilde{\varrho}) \partial_x \tilde{S} \psi + \partial_x \mathcal{S}[\tilde{\varrho}(1 - \tilde{\varrho}) \psi]\,. \tag{52}$$

In the computation of $\mathcal{L}^*$, the symmetry of the Green's function G (see (15)) has been used.

The further procedure is motivated by the following observations: With $(\tilde{\varrho}, \tilde{S})$ we have constructed a M-parameter family of approximate solutions of the steady state problem (41) producing exponentially small residuals R (see (46)). Therefore we expect

the linearized operator $\mathcal{L}$ to possess M exponentially small eigenvalues with eigenfunctions approximately given by the derivatives of $(\tilde{\varrho}, \tilde{S})$ with respect to the parameters $x_1, \ldots, x_M$. As a consequence, the inverse of $\mathcal{L}$ will only act as a bounded operator on the inhomogeneity $J + R$ in the equation for r, if this inhomogeneity satisfies M solvability conditions characterized by the eigenfunctions of $\mathcal{L}^*$ corresponding to the exponentially small eigenvalues. Since $\mathcal{L}$ is not self adjoint (the other major difference compared to earlier work for, e.g., the Cahn-Hilliard equation), the computation of approximations for these eigenfunctions is not immediate. We proceed pragmatically by trying to determine candidates for ψ, such that the terms involving the unknown r in (51) become negligibly small.

The first two terms in (52) constitute a singularly perturbed differential operator with turning points (see [9]) close to $x = x_i$ (where $\tilde{\varrho} = 1/2$) and at $x = \tilde{x}_{i+1/2}$ (the extrema of $\tilde{S}$). These turning points are of different character since the sign of the coefficient $(1 - 2\tilde{\varrho})\partial_x \tilde{S}$ changes from positive to negative close to the x_i and vice versa at the $\tilde{x}_{i+1/2}$. The second group of turning points is interesting for us, since their character allows for spike layer solutions of the differential equation

$$\varepsilon \partial_x \psi + (1 - 2\tilde{\varrho})\partial_x \tilde{S} \psi = 0 \,.$$

Such spike layer solutions will be the basis for our construction of appropriate ψs. More precisely, we choose (for $i = 1, \ldots, M-1$)

$$\psi_{i+1/2}(x) = c_{i+1/2} \exp\left(-\frac{1}{\varepsilon} \int_{\tilde{x}_{i+1/2}}^{x} (1 - 2\tilde{\varrho}(z))\partial_x \tilde{S}(z) dz \right)$$

for $x_i \le x \le x_{i+1}$. Outside of this interval we extend $\psi_{i+1/2}$ as a smooth function satisfying

$$\begin{aligned}
&\psi_{i+1/2}(x) = 0 \quad \text{for } 0 \le x \le \tilde{x}_{i-1/2} \,, \\
&|\psi_{i+1/2}(x)| \le \psi_{i+1/2}(x_i) \quad \text{for } \tilde{x}_{i-1/2} \le x \le x_i \,, \\
&|\psi_{i+1/2}(x)| \le \psi_{i+1/2}(x_{i+1}) \quad \text{for } x_{i+1} \le x \le \tilde{x}_{i+3/2} \,, \\
&\psi_{i+1/2}(x) = 0 \quad \text{for } \tilde{x}_{i+3/2} \le x \le L \,,
\end{aligned}$$

which is possible under the basic assumption of the whole asymptotic procedure that all the points x_j and $\tilde{x}_{j+1/2}$ are well separated from each other. The constant $c_{i+1/2}$ is chosen such that $\psi_{i+1/2}$ approximately becomes a Delta-family for $\varepsilon \to 0$. This involves the computation of the integral

$$\begin{aligned}
&\int_0^L \exp\left(-\frac{1}{\varepsilon} \int_{\tilde{x}_{i+1/2}}^{x} (1 - 2\tilde{\varrho}(z))\partial_x \tilde{S}(z) dz \right) dx \\
&\approx \int_{x_i}^{x_{i+1}} \exp\left(-\frac{|\partial_x^2 \tilde{S}(\tilde{x}_{i+1/2})|(x - \tilde{x}_{i+1/2})^2}{2\varepsilon} \right) dx \approx \sqrt{\frac{2\pi\varepsilon}{|\partial_x^2 \tilde{S}(\tilde{x}_{i+1/2})|}} \,,
\end{aligned}$$

leading to

$$c_{i+1/2} = \sqrt{\frac{|\partial_x^2 \tilde{S}(\tilde{x}_{i+1/2})|}{2\pi\varepsilon}} \,.$$

In this construction we have neglected the last term in the adjoint operator (52) so far. Since $\tilde{\varrho}(1-\tilde{\varrho})\psi_{i+1/2}$ is uniformly exponentially small, the same holds for $\partial_x \mathcal{S}[\tilde{\varrho}(1-\tilde{\varrho})\psi_{i+1/2}]$, and, thus, also for $\mathcal{L}^*\psi_{i+1/2}$.

Using the functions $\psi_{i+1/2}$ in (51), we have to compute

$$\int_0^L \psi_{i+1/2} J \, dx \approx J(\tilde{x}_{i+1/2}) \approx \sum_{j=1}^{i} (-1)^{k_j} \dot{x}_j \,,$$

as well as

$$\int_0^L \psi_{i+1/2} R \, dx \,.$$

The approximation of the second integral is less straightforward since, by (46), the integrand vanishes at $\tilde{x}_{i+1/2}$ where the mass of $\psi_{i+1/2}$ concentrates. We therefore split the integral into four parts A, B, C, and D, corresponding to the subintervals $(0, x_i)$, $(x_i, \tilde{x}_{i+1/2})$, $(\tilde{x}_{i+1/2}, x_{i+1})$, and (x_{i+1}, L), respectively. Using (46) and the properties of $\psi_{i+1/2}$, we easily estimate the first and the last terms:

$$\begin{aligned} |A| &\le c\psi_{i+1/2}(x_i)|\Delta\varrho_i| \,, \\ |D| &\le c\psi_{i+1/2}(x_{i+1})|\Delta\varrho_{i+1}| \,, \end{aligned}$$

with an ε-independent constant c. In a neighbourhood of $\tilde{x}_{i+1/2}$, the residual can be approximated up to an exponentially small relative error by $R \approx \Delta\varrho_i(1-2\tilde{\varrho})\partial_x\tilde{S}$ for $x < \tilde{x}_{i+1/2}$, and by $R \approx \Delta\varrho_{i+1}(1-2\tilde{\varrho})\partial_x\tilde{S}$ for $x > \tilde{x}_{i+1/2}$. For the other two subintegrals we therefore obtain

$$\begin{aligned} B &\approx c_{i+1/2}\Delta\varrho_i \int_{x_i}^{\tilde{x}_{i+1/2}} \exp\left(-\frac{1}{\varepsilon}\int_{\tilde{x}_{i+1/2}}^{x} (1-2\tilde{\varrho}(z))\partial_x\tilde{S}(z)dz\right)(1-2\tilde{\varrho}(x))\partial_x\tilde{S}(x)dx \\ &\approx -\varepsilon c_{i+1/2}\Delta\varrho_i \,, \end{aligned}$$

and, similarly,

$$C \approx \varepsilon c_{i+1/2}\Delta\varrho_{i+1} \,.$$

Since $\Delta\varrho_i$ is multiplied by the $O(\sqrt{\varepsilon})$-constant $\varepsilon c_{i+1/2}$ in B and by the exponentially small $\psi_{i+1/2}(x_i)$ in A, A is negligible compared to B and, analogously, D is negligible compared to C.

Collecting our results and using that $\psi_{i+1/2}$ vanishes on the boundary, (51) with $\psi = \psi_{i+1/2}$ leads to

$$\sum_{j=1}^{i} (-1)^{k_j} \dot{x}_j = \varepsilon c_{i+1/2}(\Delta\varrho_{i+1} - \Delta\varrho_i) \,, \tag{53}$$

for $1 \le i \le M-1$. As previously announced, a common additive constant in the $\Delta\varrho_i$ would not change this result. From (53) with $i = 1$ we obtain an ODE for x_1:

$$\dot{x}_1 = (-1)^{k_1}\varepsilon c_{3/2}(\Delta\varrho_2 - \Delta\varrho_1) \,. \tag{54}$$

Equations for x_i, $2 \le i \le M-1$, are derived by taking differences of consecutive versions of (53):

$$\dot{x}_i = (-1)^{k_i}\varepsilon \left[c_{i+1/2}(\Delta\varrho_{i+1} - \Delta\varrho_i) - c_{i-1/2}(\Delta\varrho_i - \Delta\varrho_{i-1}) \right] . \tag{55}$$

Finally, the difference between the mass conservation equation (50) and (53) with $i = M-1$ gives

$$\dot{x}_M = (-1)^{k_M}\varepsilon c_{M-1/2}(\Delta\varrho_{M-1} - \Delta\varrho_M) . \tag{56}$$

In principal, this completes the asymptotic procedure, and the dynamics of $x_1(t), \ldots, x_M(t)$ is completely determined by (54)–(56). However, the right hand sides in (54)–(56) are given in terms of $\tilde{S}$, the solution of (45), which is not known explicitly. On the other hand, it will be shown in the appendix that the explicitly computable $\bar{S}_\infty$ is a good enough approximation (essentially up to $O(\varepsilon^2)$) for $\tilde{S}$ to maintain the accuracy of the leading terms in (54)–(56). Therefore, the final result of our asymptotics is the system (54)–(56) with

$$\begin{aligned}
\Delta\varrho_{i+1} - \Delta\varrho_i &= \left[1 + \exp\left(\frac{\bar{S}_\infty(x_{i+1}) - \bar{S}_\infty(\bar{x}_{i+1/2})}{\varepsilon} \right) \right]^{-1} \\
&\quad - \left[1 + \exp\left(\frac{\bar{S}_\infty(x_i) - \bar{S}_\infty(\bar{x}_{i+1/2})}{\varepsilon} \right) \right]^{-1} , \\
c_{i+1/2} &= \sqrt{\frac{|\bar{S}_\infty(\bar{x}_{i+1/2}) - \bar{\varrho}_\infty(\bar{x}_{i+1/2})|}{2\pi\varepsilon}} , \\
\bar{S}_\infty(x) &= \sum_{k_i \text{ odd}} \int_{x_i}^{x_{i+1}} \left[\frac{1}{2} e^{-|x-y|} + \frac{e^{x+y} + e^{2L-x-y} + e^{x-y} + e^{y-x}}{2(e^{2L}-1)} \right] dy .
\end{aligned}$$

The whole asymptotic approach is based on the fact that the movement of the boundary layers is exponentially slow. It is valid only as long as x_1 and x_M stay away from the boundaries and an extremal point $\bar{x}_{i+1/2} \in (x_i, x_{i+1})$ of $\bar{S}_\infty$ exists for every pair $x_i < x_{i+1}$. These conditions are equivalent to the requirement that all plateau boundaries satisfy the entropy conditions (34). As soon as they are violated, the hyperbolic dynamics starts to dominate.

With the above approximations, the right hand sides of (54)–(56) can be evaluated explicitly in terms of $x_1, \ldots, x_M$. However, in the general case the formulas are very long and not very instructive. They involve not only the evaluation of the integrals in the last equation above, but also the computation of all the extremal points $\bar{x}_{3/2}, \ldots, \bar{x}_{M-1/2}$ of $\bar{S}_\infty$. As an example, we discuss the simplest situation $M = 2$ with $k_0 = 1$, i.e., two plateaus adjacent to the boundaries with one vacuum region in the middle. In this case, the system (54)–(56) reduces to

$$\dot{x}_1 = \dot{x}_2 = \varepsilon c_{3/2}(\Delta\varrho_2 - \Delta\varrho_1) . \tag{57}$$

Conservation of the initial mass m implies $x_1 + (L - x_2) = m$, and the system can be reduced to a scalar equation for x_1, substituting $x_2 = L - m + x_1$. The chemoattractant density is given by

$$\bar{S}_\infty(x) = \frac{\sinh(x_1)\cosh(L-x) + \sinh(m-x_1)\cosh(x)}{\sinh(L)} ,$$

for $x_1 \le x \le x_2$ with one interior minimum at

$$\bar{x}_{3/2} = \frac{1}{2} \log \frac{e^L \sinh(x_1) + \sinh(m - x_1)}{e^{-L} \sinh(x_1) + \sinh(m - x_1)} .$$

Steady states of (57) have to satisfy $\bar{S}_\infty(x_1) = \bar{S}_\infty(x_2)$. It is easily seen that $x_1 = m/2$ is the only solution, i.e., the only steady state is the symmetric one, where the mass is distributed equally between the two plateaus. In general, $\mathrm{sign}(x_1 - m/2) = \mathrm{sign}(\bar{S}_\infty(x_1) - \bar{S}_\infty(x_2)) = \mathrm{sign}(\dot{x}_1)$, showing the instability of the steady state. If initially one of the plateaus is bigger, then it will grow at the expense of the smaller one until all the mass is concentrated adjacent to one of the boundaries. This is expected to be the stable stationary state.

In the general case $M > 2$, our understanding of the qualitative behaviour of (54)–(56) is less complete. It is easy to see that steady states are characterized by the requirement that $\bar{S}_\infty$ takes the same value at the plateau edges $x_1, \ldots, x_M$. This implies that all plateaus have the same length and that the same is true for the vacuum regions separating them, with plateaus and/or vacuum regions adjacent to the boundary having half the interior length. This shows that all stationary solutions of the full problem as characterized in [13] are represented. We conjecture that all these solutions are unstable, but a proof is missing.

About the dynamics we observe that, generically, one of the exponentially small terms $\Delta\varrho_{i+1} - \Delta\varrho_i$ will dominate all the others. As a consequence, effectively only to neighbouring plateau edges x_i and x_{i+1} will move (with the same velocity), while the others are approximately stationary.

In fig. 4, we compare the numerical solution of the full system (5), (6) with the solution of system (54)-(56) by plotting the position of the boundaries of a single plateau situated at $x_1 = 0.6$ and $x_2 = 0.8$ for different values of ε. Light lines represent the solution obtained by solving the full system with an Upwind scheme with grid size $\Delta x = \Delta t = 3 \times 10^{-4}$, dark lines were obtained by solving system (54)-(56) for $M = 2$ using the MAPLE routine `lsode` (a Livermore Stiff ODE solver). The two lowest branches in the figure correspond to $\varepsilon = 4 \times 10^{-4}$, and it can be observed that the time it takes the plateau to advance towards the boundary calculated by the two different approaches differs slightly. However, as we decrease ε ($\varepsilon = 2 \times 10^{-4}$ for the middle branches, $\varepsilon = 1 \times 10^{-4}$ for the top branches) and thus the error introduced by the approximating assumptions we had to take in order to obtain the ODEs (54)-(56), the distance between the lines decreases until, for $\varepsilon = 1 \times 10^{-4}$, the trajectories of x_1 and x_2 obtained by the Upwind scheme and the ODE-system are practically identical.

5 A hybrid numerical-asymptotic approach

Developing a numerical scheme that captures both the short and the long-time behaviour of the parabolic system correctly is a non-trivial task. If we use a standard discretization of (5), (6) with a grid size that is too large, the long-time behaviour of the system will be driven by numerical errors dominating the exponentially small terms responsible for

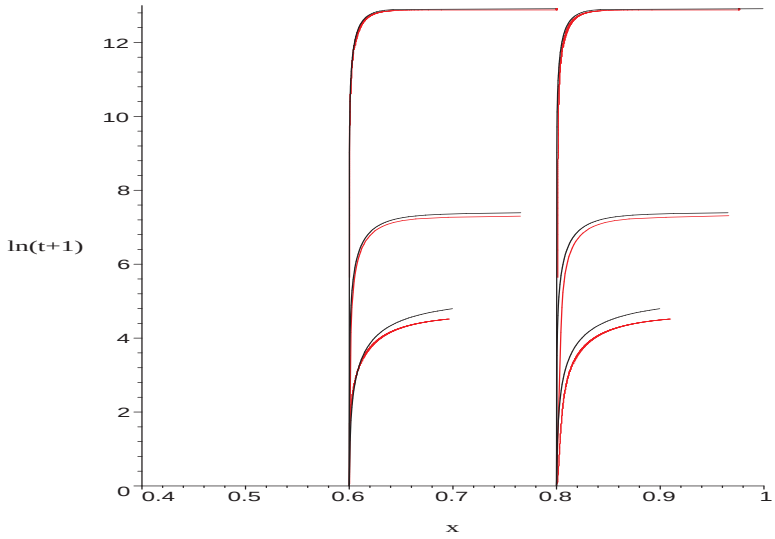

Figure 4: Comparison of the numerical solution of system (5), (6) with $\varepsilon = 4 \times 10^{-4}$, 2×10^{-4} and 1×10^{-4} obtained with an upwind-scheme (light) and the numerical solution of the corresponding ODE-system (dark). The different length of the branches is due to the fact that as ε becomes smaller, solutions keep their plateau-like shape even when they get quite close to the boundary, whereas for larger ε, the hyperbolic dynamics start to take over much faster.

the exact dynamics. Choosing a grid that is fine enough to reduce numerical errors in a sufficient way leads to very long computation times (for instance, the solution of the full system (5), (6) for fig. 3 took several days on a Linux workstation). Another approach is to solve the equations for the positions of the plateau edges (54) - (56), and then to specify an approximate solution $\tilde{\varrho}$ at each time step according to (44). However, this solution is only valid as long as the conditions (34) are satisfied.

These observations motivate a combined approach for the numerical solution of (5), (6): As long as (34) holds, we use the asymptotic approximations (54) - (56). We solve the equations with MAPLE and calculate the corresponding $\tilde{\varrho}$ at each time step. When the velocities of the plateau edges become $\mathcal{O}(\varepsilon)$, we switch to a full numerical solution with the finite difference scheme described above. A similar numerical-asymptotic approach was developed in [17] to solve the viscous Cahn-Hillard equation in one space dimension.

Example: Behaviour near a stationary state

As an example, we investigate the dynamics of the parabolic system when solutions are initially close to an unstable stationary state.

For a given initial mass m, this stationary solution consists of two plateaus of equal mass, with the outer edges being exactly half the distance between the plateaus away

from the boundaries. The stationary solution is given by

$$x_1 = \frac{L-m}{4}, \quad x_2 = \frac{L+m}{4}, \quad x_3 = \frac{3L-m}{4}, \quad x_4 = \frac{3L+m}{4}. \tag{58}$$

In our experiments, we set $m = 0.4$ and $L = 1$ to obtain the boundary layer positions $x_1 = 0.15$, $x_2 = 0.35$, $x_3 = 0.65$ and $x_4 = 0.85$ from (58). Then we choose two different sets of initial conditions close to this stationary point and calculate the temporal evolution of the boundary layers according to (54) - (56) with $M = 4$. After a plateau has moved to the domain boundary or merged with another plateau, we solve the system for $M = 3$ or $M = 2$ respectively.

In Fig. 5(a), the left plateau has initially been made smaller and moved towards the left boundary. The evolution proceeds in three steps: 1. The left plateau moves to the left, until it reaches the boundary. 2. The right plateau moves to the right boundary. 3. The two remaining plateau edges move to the left, meaning that the bigger right plateau attracts cells from the left. The evolution stops after the left plateau has disappeared and one plateau adjacent to the right boundary is left as stable steady state. As mentioned in the previous section, during each step only one pair of plateau edges moves in parallel.

Fig. 5(b) features an initial condition, where the left plateau has again been made smaller but now moved towards the center compared to the unstable steady state. We observe a two-step evolution: 1. The left plateau moves to the right until it looses stability and is absorbed by the bigger right plateau. 2. The remaining plateau moves to the right until it reaches the boundary. An animation (obtained with the combined numerical-asymptotic approach described above) corresponding to fig. 5(b) can be found at http://www.ricam.oeaw.ac.at/people/page/dolak/animation.html.

Details of the fast hyperbolic dynamics at the end of step 1 are shown in Fig. 6. As the left plateau moves towards the right one, a rarefaction wave starts to form when the entropy condition for the corresponding hyperbolic system becomes violated. The outer plateau edge of the right plateau is not affected by this merging process and does not move, since locally, the entropy condition is still satisfied. In general, however, it is an open problem to predict the outcome of the hyperbolic evolution because of the nonlocal coupling. After the loss of stability of a plateau edge, the hyperbolic evolution could induce stability losses of other plateau edges. Therefore it cannot be ruled out that several plateaus disappear within one 'hyperbolic transition layer'.

Appendix

We shall prove solvability of the approximate steady state problem (45) and an approximation result for its solution. Recalling the definition (32), (33) of the plateau state $(\bar{\varrho}_\infty, \bar{S}_\infty)$ and of the extremal points $\bar{x}_{i+1/2} \in (x_i, x_{i+1})$ of $\bar{S}_\infty$, we define

$$x_{i\pm1/4} := \frac{x_i + \bar{x}_{i\pm1/2}}{2} \quad \text{for } 1 \le i \le M\,, \qquad x_{1/4} := 0\,, \qquad x_{M+3/4} := L\,,$$

and

$$A_1 := \bigcup_{i=1}^{M} (x_{i-1/4}, x_{i+1/4})\,, \qquad A_2 := [0, L] \setminus A_1 = \bigcup_{i=0}^{M} [x_{i+1/4}, x_{i+3/4}]\,.$$

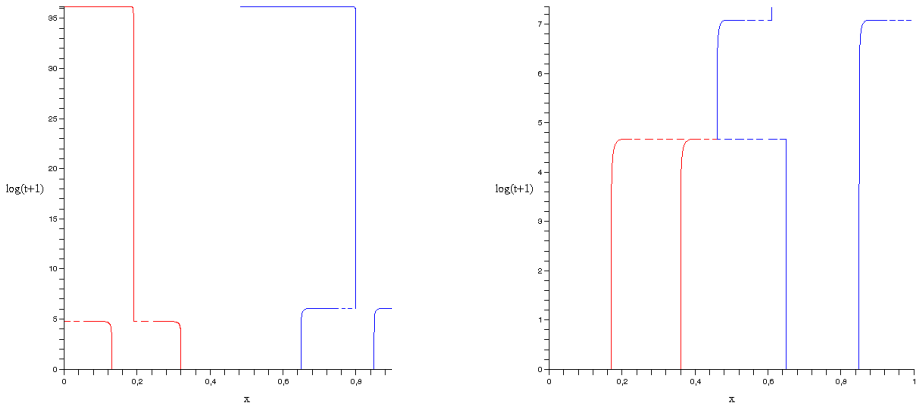

(a) $x_1 = 0.13$, $x_2 = 0.32$ (b) $x_1 = 0.15$, $x_2 = 0.36$

Figure 5: Solutions of the ODE-system (54) - (56) with different initial conditions and $\varepsilon = 2 \times 10^{-4}$. The position of the right plateau is $x_3 = 0.65$, $x_4 = 0.85$ in all pictures.

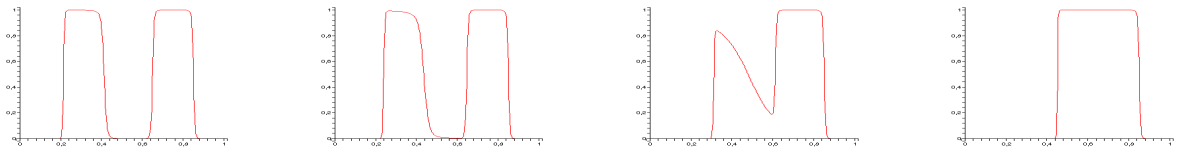

(a) $t = 48000$ (b) $t = 48130$ (c) $t = 48158$ (d) $t = 48165$

Figure 6: Fast dynamics of the parabolic system, corresponding to the dashed lines in Fig. 5(b). The first picture shows the cell density calculated according to the asymptotic approximations (54) - (56) and (44) shortly before the hyperbolic dynamics start to dominate. The middle pictures show a rarefaction wave obtained by solving (5), (6) with an upwind scheme until, as shown in the last picture, only one plateau is left.

Since A_1 stays away from the extremal points of $\bar{S}_\infty$, and A_2 stays away from its turning points x_i, there exists a $\delta > 0$ such that

$$|\partial_x \bar{S}_\infty| \geq 2\delta \quad \text{in } A_1\,, \qquad |\partial_x^2 \bar{S}_\infty| \geq 2\delta \quad \text{in } A_2\,.$$

For chemoattractant densities we shall use the Banach space $\mathcal{B}_1 := C^1([0,L]) \cap C^2(A_2)$ with its natural norm

$$\|S\|_1 := \|S\|_{L^\infty((0,L))} + \|\partial_x S\|_{L^\infty((0,L))} + \|\partial_x^2 S\|_{L^\infty(A_2)}\,,$$

and the ball

$$B_\delta := \{S : \ \|S - \bar{S}_\infty\|_1 < \delta\}\,.$$

Then $S \in B_\delta$ implies

$$|\partial_x S| \geq \delta \quad \text{in } A_1\,, \qquad |\partial_x^2 S| \geq \delta \quad \text{in } A_2\,.$$

Therefore, in every subinterval $[x_{i+1/4}, x_{i+3/4}]$ of A_2, S has a unique local extremum $x_{i+1/2}[S]$ of the same character as $\bar{x}_{i+1/2} = x_{i+1/2}[\bar{S}_\infty]$. Consequently $\tilde{\varrho}[S]$ is well defined by (44). A fixed point operator for solving (45) is now defined on B_δ by

$$F[S](x) := \mathcal{S}[\tilde{\varrho}[S]]\,. \tag{59}$$

Our Banach space for cell densities will be $\mathcal{B}_2 := L^1((0,L)) \cap C(A_2)$ with the norm

$$\|\varrho\|_2 := \|\varrho\|_{L^1((0,L))} + \|\varrho\|_{L^\infty(A_2)}\,.$$

First we prove that the map $\mathcal{S}$ from ϱ to S given by solving the elliptic S-problem is continuous.

Lemma 5.1 *There exists a $c > 0$ such that for every $\varrho \in \mathcal{B}_2$, $\mathcal{S}[\varrho] \in \mathcal{B}_1$ holds and $\|\mathcal{S}[\varrho]\|_1 \leq c\|\varrho\|_2$.*

Proof. The result is a consequence of the facts that G and $\partial_x G$ are uniformly bounded and that $S = \mathcal{S}[\varrho]$ solves the differential equation $\partial_x^2 S = S - \varrho$. □

Now we are ready to prove the main result of this section.

Theorem 5.2 *For ε small enough, the problem (45) has a unique solution in B_δ.*

Proof. For every $S \in B_\delta$, $\tilde{\varrho}[S]$ deviates from $\bar{\varrho}_\infty$ only by boundary layer corrections close to the discontinuities $x_1, \ldots, x_M \in A_1$. The thickness of the boundary layers is $O(\varepsilon)$. In A_2, $\tilde{\varrho}[S]$ and $\bar{\varrho}_\infty$ are exponentially close as $\varepsilon \to 0$. This immediately implies $\|\tilde{\varrho}[S] - \bar{\varrho}_\infty\|_2 = O(\varepsilon)$ and, thus, from Lemma 5.1, $\|F[S] - \bar{S}_\infty\|_1 = O(\varepsilon)$. This proves that for ε small enough, F maps B_δ into itself.

Now let $S_1, S_2 \in B_\delta$ and set $x^l_{i+1/2} := x_{i+1/2}[S_l]$, $\hat\varrho^l_i := \hat\varrho_i[S_l]$, $\Delta\varrho^l_i := \Delta\varrho_i[S_l]$, $l = 1, 2$. Assume $\partial_x S_1(x_i), \partial_x S_2(x_i) > 0$ and $x_i < x < \min\{x^1_{i+1/2}, x^2_{i+1/2}\}$. Then we have

$$\begin{aligned}
|\hat\varrho^1_i(x) - \hat\varrho^2_i(x)| &\leq \left|\exp\left(\frac{S_1(x_i) - S_1(x)}{\varepsilon}\right) - \exp\left(\frac{S_2(x_i) - S_2(x)}{\varepsilon}\right)\right| \\
&\leq \exp\left(\frac{\delta(x_i - x)}{\varepsilon}\right)\frac{1}{\varepsilon}\left|S_1(x_i) - S_1(x) - S_2(x_i) + S_2(x)\right| \\
&\leq \exp\left(\frac{\delta(x_i - x)}{\varepsilon}\right)\frac{x - x_i}{\varepsilon}\|S_1 - S_2\|_1 .
\end{aligned}$$

Analogous estimates for $\max\{x^1_{i-1/2}, x^2_{i-1/2}\} < x < x_i$ and for $\partial_x S_l(x_i) < 0$ lead to

$$|\hat\varrho^1_i(x) - \hat\varrho^2_i(x)| \leq \exp\left(-\frac{\delta|x_i - x|}{\varepsilon}\right)\frac{|x - x_i|}{\varepsilon}\|S_1 - S_2\|_1 , \tag{60}$$

for $1 \leq i \leq M$ and $\max\{x^1_{i-1/2}, x^2_{i-1/2}\} < x < \min\{x^1_{i+1/2}, x^2_{i+1/2}\}$.

The mean value theorem gives

$$\partial_x S_1(x^2_{i+1/2}) - \partial_x S_2(x^2_{i+1/2}) = \partial_x S_1(x^2_{i+1/2}) = \partial^2_x S_1(\xi_{i+1/2})(x^2_{i+1/2} - x^1_{i+1/2}) ,$$

with $\xi_{i+1/2} \in A_2$. Since $S_1 \in B_\delta$,

$$|x^1_{i+1/2} - x^2_{i+1/2}| \leq \frac{1}{\delta}\|S_1 - S_2\|_1 \tag{61}$$

follows. Now assume $x^1_{i+1/2} < x^2_{i+1/2}$. Then we can estimate

$$|\hat\varrho^1_i(x^1_{i+1/2}) - \hat\varrho^2_i(x^2_{i+1/2})| \leq |\hat\varrho^1_i(x^1_{i+1/2}) - \hat\varrho^2_i(x^1_{i+1/2})| + |\hat\varrho^2_i(x^1_{i+1/2}) - \hat\varrho^2_i(x^2_{i+1/2})| .$$

For the first term on the right hand side, (60) can be used to give a bound of the form $\mathcal{EST}\|S_1 - S_2\|_1$, where the abbreviation $\mathcal{EST}$ means 'exponentially small term', i.e., a term of the form $\exp(-\kappa/\varepsilon)$ with $\kappa > 0$. For the second term we use (61) and the fact that $\partial_x\hat\varrho^2_i$ is exponentially small in A_2 to obtain an estimate of the same type. Interchanging the roles of S_1 and S_2, the same can be done for $x^2_{i+1/2} < x^1_{i+1/2}$. A consequence of these results is

$$|\Delta\varrho^1_i - \Delta\varrho^2_i| \leq \mathcal{EST}\|S_1 - S_2\|_1 \tag{62}$$

for $1 \leq i \leq M$. Combining (60) and (62), we have

$$|\tilde\varrho[S_1](x) - \tilde\varrho[S_2](x)| \leq \left[\mathcal{EST} + \exp\left(-\frac{\delta|x_i - x|}{\varepsilon}\right)\frac{|x - x_i|}{\varepsilon}\right]\|S_1 - S_2\|_1 , \tag{63}$$

for $1 \leq i \leq M$ and $\max\{x^1_{i-1/2}, x^2_{i-1/2}\} < x < \min\{x^1_{i+1/2}, x^2_{i+1/2}\}$. It remains to consider $\eta_{i+1/2} := \min\{x^1_{i+1/2}, x^2_{i+1/2}\} < x < \max\{x^1_{i+1/2}, x^2_{i+1/2}\}$:

$$|\tilde\varrho[S_1](x) - \tilde\varrho[S_2](x)| \leq |\tilde\varrho[S_1](\eta_{i+1/2}) - \tilde\varrho[S_2](\eta_{i+1/2})| + \mathcal{EST}|x - \eta_{i+1/2}| ,$$

since $\partial_x \tilde{\varrho}[S_l]$ is exponentially small in A_2. For the first term on the right hand side we use (63) and for the second (61), to obtain

$$|\tilde{\varrho}[S_1](x) - \tilde{\varrho}[S_2](x)| \leq \mathcal{ESTL}\|S_1 - S_2\|_1\,, \tag{64}$$

for $0 \leq i \leq M$ and $\min\{x^1_{i+1/2}, x^2_{i+1/2}\} < x < \max\{x^1_{i+1/2}, x^2_{i+1/2}\}$. Since the integral of the second term in the bracket in (63) is $O(\varepsilon)$, a combination of (63) and (64) leads to

$$\|\tilde{\varrho}[S_1] - \tilde{\varrho}[S_2]\|_2 \leq c\,\varepsilon\|S_1 - S_2\|_1\,,$$

and, with Lemma 5.1,

$$\|F[S_1] - F[S_2]\|_1 \leq c\,\varepsilon\|S_1 - S_2\|_1\,,$$

showing that F is a contraction for ε small enough and, thus, completing the proof of the theorem. □

Finally, it will be shown by formal asymptotic arguments that it is asymptotically correct to approximate $\tilde{S}$ by $\bar{S}_\infty$ in the right hand sides of the ODEs (54)–(56). It is easily seen that the exponentially small terms in the $\Delta\varrho_i$ are approximated with a $O(\varepsilon)$ relative error if the chemoattractant density $\tilde{S}$ is approximated up to $O(\varepsilon^2)$. This holds for $\bar{S}_\infty$ since

$$\begin{aligned}
\tilde{S}(x) - \bar{S}_\infty(x) &= \int_0^L G(x,y)(\tilde{\varrho}[\tilde{S}](y) - \bar{\varrho}_\infty(y))dy \\
&= \sum_{i=1}^{M} \int_{\tilde{x}_{i-1/2}}^{\tilde{x}_{i+1/2}} G(x,y)(\hat{\varrho}_i[\tilde{S}](y) - \bar{\varrho}_\infty(y) - \Delta\varrho_i)dy \\
&= \varepsilon \sum_{i=1}^{M} (-1)^{k_i} G(x,x_i)\left(\int_0^\infty \frac{d\xi}{1+\exp(|\partial_x \tilde{S}(x_i)|\xi)} \right. \\
&\qquad \left. - \int_{-\infty}^0 \frac{d\xi}{1+\exp(-|\partial_x \tilde{S}(x_i)|\xi)} \right) + O(\varepsilon^2) \\
&= O(\varepsilon^2)\,.
\end{aligned}$$

The third equality is due to the substitution $y = x_i + \varepsilon\xi$ and straightforward Taylor expansion.

Acknowledgements. Y.D. wants to thank T. Hillen for valuable discussions. The authors also owe thanks to two anonymous referees, whose comments motivated major improvements in this work, which has been supported financially by the Austrian Science Foundation, grant nos. W008 and P16174-N05, and by the European HYKE network.

References

[1] P. Bates and J. Xun. Metastable patterns for the Cahn-Hilliard equation I. *J. Differential Equations*, 2(111):421–457, 1994.

[2] P. Bates and J. Xun. Metastable patterns for the Cahn-Hilliard equation II. Layer dynamics and slow invariant manifold. *J. Differential Equations*, 1(117):165–216, 1995.

[3] Y. Dolak and C. Schmeiser. Kinetic models for chemotaxis: Hydrodynamic limits and the back-of-the-wave problem. *J. Math. Biol.*, 2005.

[4] J. Haskovec and C. Schmeiser. Transport in semiconductors at saturated velocities. ANUM Preprint.

[5] T. Hillen and K. Painter. Global existence for a parabolic chemotaxis model with prevention of overcrowding. *Adv. in Appl. Math.*, 26(4):280–301, 2001.

[6] E.F. Keller and L.A. Segel. Initiation of slime mold aggregation viewed as an instability. *J. Theor. Biol.*, 26:399–415, 1970.

[7] J. Laforgue and R. O'Malley. Shock layer movement for Burgers' equation. *SIAM J. Appl. Math.*, 55(2):332–347, 1995.

[8] P.A. Markowich and P. Szmolyan. A system of convection-diffusion equations with small diffusion coefficient arising in semiconductor physics. *J. Differential Equations*, 81:234–254, 1989.

[9] R. E. O'Malley. *Introduction to singular perturbations*. Academic Press, 1974.

[10] K. Painter and T. Hillen. Volume-filling and quorum sensing in models for chemosensitive movement. *Canad. Appl. Math. Quart.*, 10(4):280–301, 2003.

[11] C.S. Patlak. Random walk with persistence and external bias. *Bull. Math. Biophys.*, 15:311–338, 1953.

[12] A. Pazy. *Semigroups of Linear Operators and Applications to Partial Differential Equations*. Springer, New York, 1983.

[13] A.B. Potapov and T. Hillen. Metastability in chemotaxis models. *J. Dyn. Diff. Eq.*, 17, 2005.

[14] L. Reyna and M. Ward. On the exponentially slow motion of a viscous shock. *Comm. Pure Appl. Math.*, 48(2):79–120, 1995.

[15] J. Simon. Compact sets in the space $L^p(0,T;B)$. *Anal. Math. Pura Appl.*, 146:65–96, 1987.

[16] B. Sleeman, M. Ward, and J. Wei. Existence, stability and dynamics of spike patterns in a chemotaxis model. *in print*.

[17] X. Sun and M. Ward. The dynamics and coarsening of interfaces for the viscous cahn-hilliard equation in one-spatial dimension. *Studies Appl. Math.*, 105(3):203–234, 2000.

[18] M. Ward. Dynamic metastability and singular perturbations. In Michel C. Delfour, editor, *Boundaries, Interfaces, and Transitions, CRM Proc. Lecture Notes*, volume 13, pages 237–263, AMS, Providence, R.I., 1998.

[19] M. Ward. Exponential asymptotics and convection-diffusion-reaction models. *Analyzing Multiscale Phenomena Using Singular Perturbation Methods, Proceedings of Symposia in Applied Mathematics*, 56:151–184, 1998.